ALGEBRAIC SOLUTION TO THE PLANAR RIGID BODY IMPACT PROBLEM

by

DREW MORGAN

Presented to the Faculty of the Graduate School of
The University of Texas at Arlington in Partial Fulfillment
of the Requirements
for the Degree of

MASTER OF SCIENCE IN MECHANICAL ENGINEERING

THE UNIVERSITY OF TEXAS AT ARLINGTON

May 2011

ACKNOWLEDGEMENTS

I thank my advisor Dr. Alan Bowling for his encouragement and advice as I worked on this research, and for providing me with good context for my thoughts. I also thank Dr. Daejong Kim for the time he's taken to be on my committee.

I would like to thank Dr. Frank Lewis as well, for being on my committee and for employing me during my graduate studies. With him, I also thank the other students in his ACS lab, especially Emanuel Stingu, Matt Middleton, and Isaac Weintraub, who taught me almost as much as my classes did.

I would also like to thank Dr. John Ridgely for his encouragement and advice during the end of my undergraduate studies, for introducing me to modern mobile robotics, and for encouraging me to pursue a graduate degree.

Lastly, I thank Mel for her endless encouragement and support, and for being proud of me; and my parents, whose diligent support and training when I was young will be continue to be fruitful for unknowable years to come.

April 6, 2011

ABSTRACT

ALGEBRAIC SOLUTION TO THE PLANAR
RIGID BODY IMPACT PROBLEM

DREW MORGAN, M.S.

The University of Texas at Arlington, 2011

Supervising Professor: Alan Bowling

For systems of rigid bodies that undergo impacts, a series of closed-form equations are developed to solve for post-impact velocities which simulate a real-world (energy-consistent) interaction. The analysis is based in the impulse domain, and requires that the surface interaction be characterizable by Coulomb friction and an energetic coefficient of restitution. No iteration, optimization, or numerical methods are used.

TABLE OF CONTENTS

LIST OF FIGURES

CHAPTER 1

INTRODUCTION

The field of classical mechanics is one of the oldest and most well-developed in physics and engineering. The movement of masses under the influence of forces is well-understood, and many methods are available for simulating the motions of systems of masses. These methods provide tractable solutions and simulations for many real-world systems. However, most of these methods require that a rigid-body assumption be made: every point in a body is fixed with respect to every other point. If the deformation of bodies must be taken into account, a whole field of study becomes involved to characterize and quantify them.

The rigid-body assumption allows for efficient, tractable, versatile simulation of objects in motion for many real-world systems. However, a common problem occurs in these rigid-body systems: objects collide. When one rigid body hits another rigid body, a shortcoming of the rigid-body assumption jumps into apparency: the velocity of the impacting points must change instantaneously, or else their motion will carry them into an intersecting state. A discontinuity in velocity requires an infinite acceleration, which requires an infinite force to produce it.

Another way to look at the problem is this: bodies may be considered rigid as long as the forces acting on them are sufficiently small as to not deform them very much. Many real systems satisfy this approximation during *almost* every part of their motion, but violate it wildly during very brief periods when two bodies are in colliding contact. Impact forces are generated which are orders of magnitude higher than any other forces experienced by the bodies during their motion.

Thus rigid-body dynamics alone cannot explain impacts or collisions between bodies in a system. All the phenomena that may be observed during collisions of real objects (rebound, energy loss, acquisition of rotation, breaking, etc.) are due to deformations near the impacting surfaces. Many methods have been proposed to augment rigid-body dynamics, to produce these effects without requiring that bodies be considered flexible throughout the simulation.

Generally, the rigid body impact problem is handled in one of two ways: using a continuous method or a discontinuous method.[6] In continuous methods, the time-varying impact forces are calculated along with the other forces and accelerations of the rigid body system (based on some surface deformation model), and applied to the impact point only during appropriate intervals in the rigid body dynamics integration. In discontinuous methods, the impact event is considered to be very short, such that the integration of all the contact forces may become a single impulse. This impulse is applied at the instant of contact by pausing the rigid body dynamics integration, calculating a velocity change, and restarting the integration with changed velocities.

Continuous methods, such as in [11] and [4], can present a number of problems. Depending on the implementation, some problems can include induced chatter, unrealistically large surface deformations, and slow calculation times. This work avoids such problems by using a discontinuous method, most similar to Mirtich's work in [10], which utilizes a differential approach. [13] This means that the impact event, while discontinuous in time, is treated as continuous in impulse: in an instant, impulse is applied to the contacting point in a steadily increasing fashion beginning from zero, allowing velocity change to be described differentially per unit impulse. Other discontinuous methods, such as in [2], use optimization or iteration instead of a differential approach, assuming nothing about the way in which impulses are applied. Complementarity conditions are also often employed in algebraic methods. [9] [1]

Although discontinuous, differential approaches serve as the most direct foundation for this work, it diverges from them in that it substitutes an exact analytical integration for others' numerical integrations. The integration is thus performed in the derivation, leaving the calculation of the algorithm as purely algebraic. This work also differs from other discontinuous, algebraic approaches in that no optimization or iteration is required, nor must a complementarity problem be solved. From quantities available in the rigid body equations of motion, and from a pre-impact velocity state, one to three intermediate velocity states are calculated, from which the final, post-impact velocity is produced.

The analysis of this work is based on impulses applied in a plane to a point of contact during a collision, which cause instantaneous changes in velocity. The impacting surfaces are modeled using an energetic coefficient of restitution and Coulomb friction. The equations of motion for a rigid body system are simplified by integration through a short time of impact, during which the configuration of the system is assumed to be constant. To supplement this simple collision equation, a novel expression is developed for the energy exchange that occurs during the impact, guaranteeing the energy-consistency of the method.

Because this solution ties the governing equations so tightly into an algorithm, it is most clear to derive them in the context of the algorithm. Chapter 2 covers these derivations while explaining the significance and necessity of each equation. The derivation is in the most general terms possible.

To supplement the general derivation of Chapter 2, Chapter 3 provides some insight into what the actual numerical calculations look like for a specific mechanism and a specific collision. It also covers some dilemmas that are not immediately obvious, and some special cases that may occur when writing computer code for an implementation of this method.

The most obvious limitation of this method is the requirement that collision impulses be constrained to lie in a plane. Chapter 4 explains more about why this limitation exists. It also provides an incomplete derivation for full 3D impacts and presents the algorithm that would be used to solve them.

Chapter 5 offers a brief conclusion, and suggestions for future work.

CHAPTER 2

ALGORITHM AND DERIVATION

2.1 Example Mechanism

A planar double pendulum system provides a simple context to explain this method. The pendulum is composed of two equally-sized slender bars of length r and mass m hanging from a fixed support, with pin joints forming the connections. A fixed floor is placed such that it interferes with the full range of motion of the lower bar, and the colliding surface interaction is assumed to be characterizable by a coefficient of friction μ and an energetic coefficient of restitution e_*.

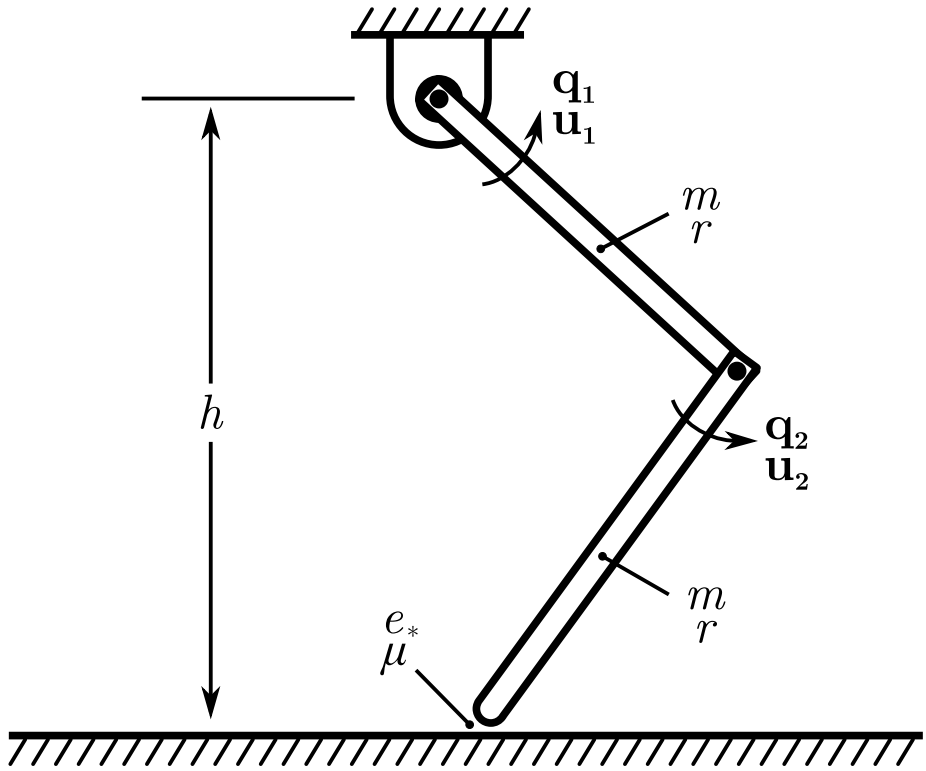

Figure 2.1. A planar double pendulum that interferes with the floor.

The equations of motion for the double-pendulum system in Figure 2.1 may be represented with generalized coordinates $\mathbf{q}$ and and generalized speeds $\mathbf{u} = \dot{\mathbf{q}}$ as: [7]

$$\mathbf{M}(\mathbf{q})\dot{\mathbf{u}} = \mathbf{b}(\mathbf{q}, \mathbf{u}) + \mathbf{g}(\mathbf{q}) + \mathbf{J}(\mathbf{q})^T\mathbf{f} \tag{2.1}$$

For reference, this mechanism has

$$\mathbf{J} = \begin{bmatrix} -\sin(\mathbf{q}_1) - \sin(\mathbf{q}_1 + \mathbf{q}_2) & -\sin(\mathbf{q}_1 + \mathbf{q}_2) \\ \cos(\mathbf{q}_1) + \cos(\mathbf{q}_1 + \mathbf{q}_2) & \cos(\mathbf{q}_1 + \mathbf{q}_2) \end{bmatrix} r$$

$$\mathbf{M} = \begin{bmatrix} \cos(\mathbf{q}_2) + \frac{5}{3} & \frac{\cos(\mathbf{q}_2)}{2} + \frac{1}{3} \\ \frac{\cos(\mathbf{q}_2)}{2} + \frac{1}{3} & \frac{1}{3} \end{bmatrix} mr^2$$

2.2 Algorithm

2.2.1 Governing Equations

The analysis of this work is based on a fundamental idea that the velocity change occurring during a collision happens in a continuous, piecewise-linear fashion with respect to a scalar impulse measurement. Within the instant of the collision, impulse is added monotonically from zero to some final value, and the generalized speeds change linearly in response to added impulse. In order to show this, a collision governing equation is derived.

A short collision duration is assumed, such that configuration of the system is approximately constant during the impact event. The generalized speeds are bounded between pre-impact and post-impact values. With these provisions, integrating (2.1) through a very short change in time Δt destroys the influence of the terms that depend only on $\mathbf{q}$ and $\mathbf{u}$. As Δt goes to zero, all that remain are a large contact force

and its associated large acceleration, which form an instantaneous impulse and its associated instantaneous velocity change.

$$\int_{\mathbf{\Delta t}} \mathbf{M}(\mathbf{q})\dot{\mathbf{u}}\,\mathrm{d}t = \int_{\Delta t} \mathbf{b}(\mathbf{q},\mathbf{u})\,\mathrm{d}t + \int_{\Delta t} \mathbf{g}(\mathbf{q})\,\mathrm{d}t + \int_{\Delta t} \mathbf{J}(\mathbf{q})^T\,\mathbf{f}\,\mathrm{d}t \tag{2.2}$$

$$\mathbf{M}\Delta\mathbf{u} = 0 + 0 + \mathbf{J}^T\mathbf{p} \tag{2.3}$$

The Jacobian matrix $\mathbf{J}$ transforms between generalized coordinates and the world coordinates of the impact point. However, the impact impulse $\mathbf{p}$ is more intuitive when expressed in a normal-tangential frame at the impact surface. Rearranging:

$$\Delta\mathbf{u} = \mathbf{M}^{-1}\mathbf{J}^T\mathbf{p} \tag{2.4}$$

The combined constants $\mathbf{M}^{-1}\mathbf{J}^T$ are called $\mathbf{L}$, the collision matrix.

$$\Delta\mathbf{u} = \mathbf{L}\mathbf{p} \tag{2.5}$$

In the general 3D case, $\mathbf{p}$ will be a vector with three components: one normal to the impact surface and two tangential to it. If the motion of the impact point is constrained to lie in a plane that contains the surface normal, whether by virtue of the whole mechanism being planar, or by means of other constraints, then the scalar tangential force during the collision is, according to dynamic Coulomb friction,

$$f_t = \pm\mu f_n \tag{2.6}$$

It may be shown [8] [3] that, after the integration into impulse space, this relation still holds:

$$p_t = \pm\mu p_n \tag{2.7}$$

The collision matrix may be split into its two columns, which multiply the normal and tangential forces separately. In the case of a 3D system where the impact

velocity is constrained to be planar, $\mathbf{L}$ will have three columns, but the impact point coordinate system may be chosen such that it is aligned in the plane of possible velocities. In this way, one of the tangential columns of $\mathbf{L}$ will multiply with the excluded impulse component, and will therefore not appear in the expansion of (2.5):

$$\Delta\mathbf{u} = \mathbf{L}_n p_n + \mathbf{L}_t p_t \tag{2.8}$$

Substituting from (2.7),

$$\begin{aligned} \Delta\mathbf{u} &= \mathbf{L}_n p_n + \mathbf{L}_t \left(\pm\mu p_n\right) \\ \Delta\mathbf{u} &= \left(\mathbf{L}_n \pm \mu\mathbf{L}_t\right) p_n \end{aligned} \tag{2.9}$$

Thus the exact velocity change caused by the instantaneous collision may be represented as a function of the magnitude of the normal impulse. All velocity change will occur along a line determined by a vector $\mathcal{L} = \mathbf{L}_n \pm \mu\mathbf{L}_t$, away from the initial velocity state $\mathbf{u}_0$.

The two components of $\mathcal{L}$ are shown In Figure 2.2, indicating the direction in which the velocity will change from the initial condition. This line will somewhere intersect a hyperplane where the normal impact velocity $\mathbf{v}_n$ is zero. It may also intersect the hyperplane where the tangential impact velocity $\mathbf{v}_t$ is zero.

The two hyperplane intersections in Figure 2.3 may be easily found algebraically once the collision line is known. The order in which these two points occur determines the order of the next calculations.

2.2.2 Friction Direction

The sign in (2.9) is determined by the direction of the frictional forces. The governing principle here is also from the continuous understanding of collisions: at every point during a collision, the friction force must be opposed to the tangential

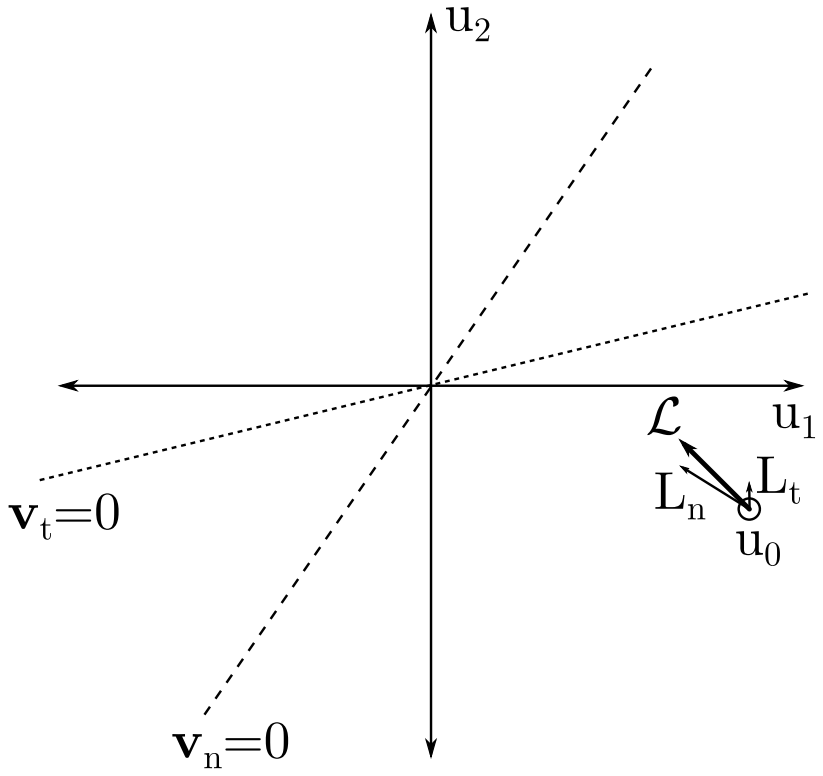

Figure 2.2. Initial collision direction.

velocity. Thus the sign in (2.9) should be positive if the tangential contact velocity is negative, and vice versa. (The vector shown in Figure 2.2 is taken with the positive sign.)

The case when the tangential velocity is exactly zero yields no direction information for the friction forces. This may correspond to a simple transition from one sign to the other, or to a sticking condition. The transition condition may be passed over while switching between the positive and negative signs, because no finite velocity change occurs at this single velocity state. The sticking condition requires special treatment.

In a dynamic friction model, the friction force is fully defined by the normal force, the coefficient of dynamic friction, and the slip velocity direction. In the static

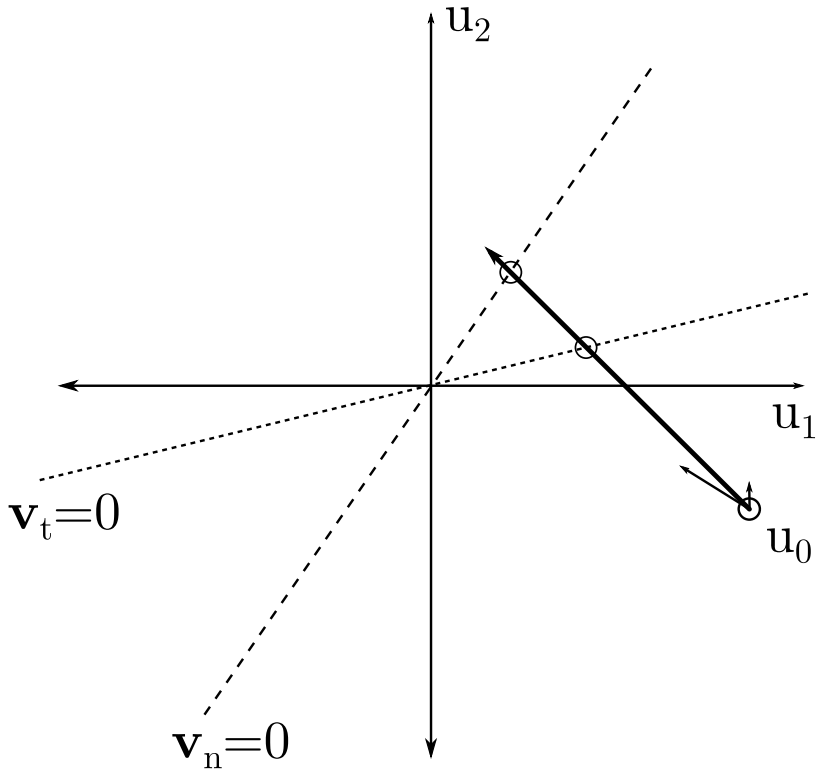

Figure 2.3. Ordering the normal and tangential pauses.

friction model, however, the equality becomes an inequality with some unknown proportion m between the magnitudes of the normal force and the friction force. The static versions of (2.6) and (2.7) are thus

$$f_t = mf_n : m \leq \mu \tag{2.10}$$

$$p_t = mp_n : m \leq \mu \tag{2.11}$$

In this analysis, m may be determined by noting that, for sticking to occur, any $\Delta\mathbf{u}$ must again yield a tangential velocity of zero. The set of all such points in $\mathbf{u}$ is the hyperplane $\mathbf{J}_a\mathbf{u} = 0$, where $\mathbf{J}_a$ denotes the first row of $\mathbf{J}$. So m is the value for which $\mathbf{L}_n + m\mathbf{L}_t$ lies within this hyperplane. It may be thought of as the required portion of the maximum available friction force to hold the sticking condition.

Thus (2.9) may be expanded as

$$\Delta\mathbf{u} = \mathcal{L}\, p_n : \qquad \mathcal{L} = \begin{cases} (\mathbf{L}_n + \mu\mathbf{L}_t) & \text{if} \quad \mathbf{J}_a\mathbf{u} < 0 \\ (\mathbf{L}_n - \mu\mathbf{L}_t) & \text{if} \quad \mathbf{J}_a\mathbf{u} > 0 \\ (\mathbf{L}_n + m\mathbf{L}_t) & \text{if} \quad \mathbf{J}_a\mathbf{u} = 0 \end{cases} \tag{2.12}$$

Because of the linear nature of (2.12), any evolution of the generalized speeds will be a piecewise straight line that crosses the hyperplane $\mathbf{J}_a\mathbf{u} = 0$ at most one time, bending at the intersection. In the case of sticking, the velocity evolution stays *within the hyperplane* after touching it.

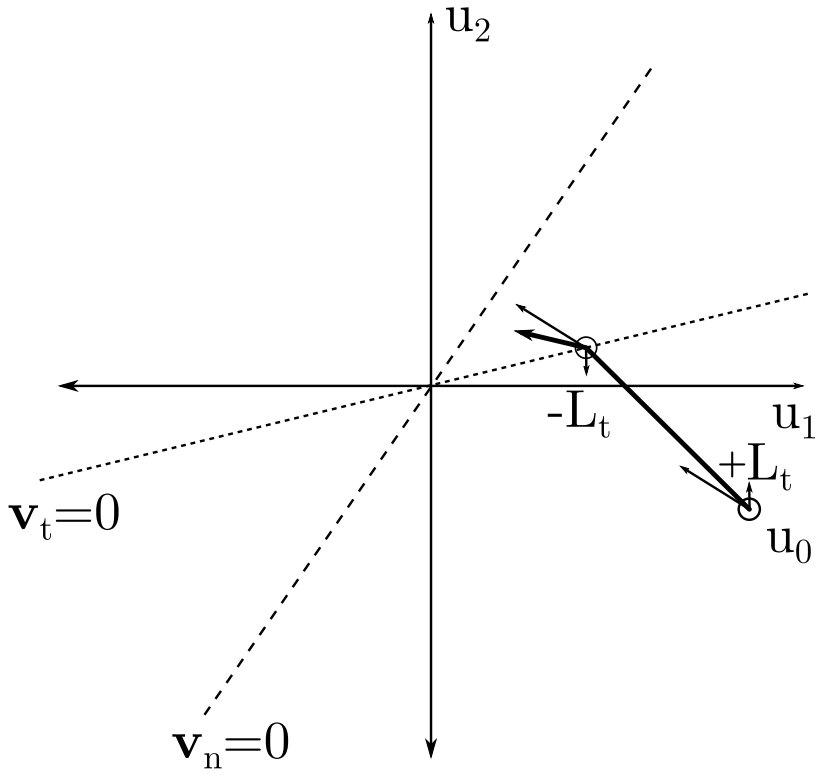

Figure 2.4. Accounting for a change in friction force direction.

The bend in the piecewise-linear trajectory at the intersection with $\mathbf{v}_t = 0$ occurs when the sign changes in (2.12). As seen in Figure 2.4, the frictional component

of the collision vector changes sign, causing $\mathcal{L}$ to point in a new direction. In this case, the originally calculated location of the $\mathbf{v}_n = 0$ intersection is not valid. It must be found again using the new collision direction, as shown in Figure 2.5. This repeated-calculation will occur at most once during any collision solution.

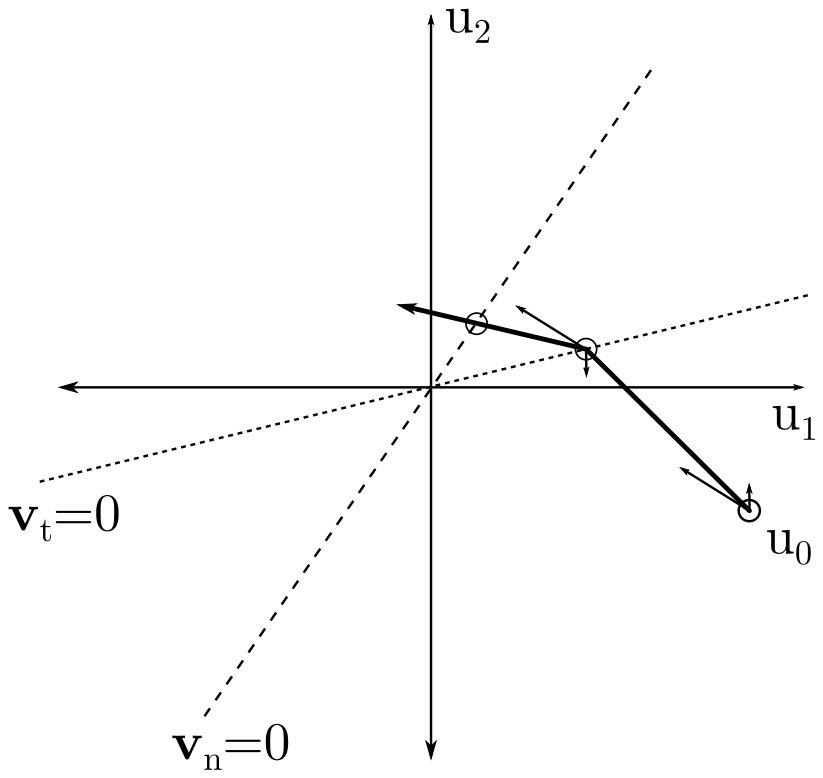

Figure 2.5. Recalculating the intersection with $\mathbf{v}_n = 0$.

2.2.3 Energetic Stopping Criterion

The $\mathbf{v}_n = 0$ intersection represents the point at which the normal velocity changes from negative (toward the impacting surface) to positive (away from the impacting surface). This point is important because of the energetic coefficient of restitution (COR), a convenient and meaningful way to determine the magnitude of p_n that simulates a real interaction between two surfaces. [12] The energetic COR may

be thought of as a measurement of how much energy is lost when a pair of surfaces compress into each other and then rebound. Energy is stored during the compression phase, and some of that energy is released during the expansion phase. The energetic COR used here is the ratio of the work done *on the compressing surfaces* to the work done *by the expanding surfaces*.

To formulate a stopping criterion based on the COR, the energy exchange of the collision must be divided into two parts: that energy which is stored briefly in compression of the impacting surfaces, and that energy which is turned into heat by sliding friction, from whence there is no restitution to the kinetic energy of the system.

The instantaneous kinetic energy of the system is given by

$$K \equiv \frac{1}{2}\mathbf{u}^T\mathbf{M}\mathbf{u} \tag{2.13}$$

Because the configuration $\mathbf{q}$ does not change during the instantaneous collision, no gravitational or other position-based potential energy is lost or gained by the rigid bodies. Instead, the only energy exchange is between kinetic energy in the system and potential energy in the (infinitesimally) compressed surfaces. The change in kinetic energy from the initial value K_i up to some point during the collision is given by

$$E \equiv \frac{1}{2}\mathbf{u}^T\mathbf{M}\mathbf{u} - K_i \tag{2.14}$$

and the derivative of E by p_n is

$$\frac{\mathrm{d}E}{\mathrm{d}p_n} = \mathbf{u}^T\mathbf{M}\frac{\mathrm{d}\mathbf{u}}{\mathrm{d}p_n} \tag{2.15}$$

The impulse derivative of (2.9),

$$\frac{\mathrm{d}\mathbf{u}}{\mathrm{d}p_n} = \mathbf{L}_n \pm \mu\mathbf{L}_t \tag{2.16}$$

may be substituted into (2.15) as

$$\frac{\mathrm{d}E}{\mathrm{d}p_n} = \mathbf{u}^T\mathbf{M}\left(\mathbf{L}_n \pm \mu\mathbf{L}_t\right) \tag{2.17}$$

This allows splitting $\mathrm{d}E/\mathrm{d}p_n$ into two parts by splitting $\mathrm{d}\mathbf{u}/\mathrm{d}p_n$ into its two parts: a "rate" of work due to the normal impulse and a "rate" of work due to the frictional impulse:

$$\begin{aligned}\frac{\mathrm{d}E}{\mathrm{d}p_n} =& \frac{\mathrm{d}_nE}{\mathrm{d}p_n} + \frac{\mathrm{d}_fE}{\mathrm{d}p_n}\\ \frac{\mathrm{d}_nE}{\mathrm{d}p_n} \equiv& \mathbf{u}^T\mathbf{M}\mathbf{L}_n \qquad (2.18)\\ \frac{\mathrm{d}_fE}{\mathrm{d}p_n} \equiv& \pm\mu\mathbf{u}^T\mathbf{M}\mathbf{L}_t \qquad (2.19)\end{aligned}$$

The normal impulse portion, governed by the energetic COR may be positive or negative, while the frictional portion must always extract kinetic energy from the system without yielding it back. E is defined as an energy exchange or work rate in this way because it can represent either a loss of kinetic energy in the rigid bodies, or a gain in potential energy (compressive or thermal) of the contacting surfaces.

Into each of these parts of E, the instantaneous generalized speeds may be substituted from (2.9). The normal part, (2.18), becomes

$$\frac{\mathrm{d}_nE}{\mathrm{d}p_n} = \left[\mathbf{u}_o + \left(\mathbf{L}_n \pm \mu\mathbf{L}_t\right)p_n\right]^T\mathbf{M}\mathbf{L}_n \tag{2.20}$$

This partial work rate may then be integrated through p_n to break the total exchanged energy E into two distinct parts: a normal part E_n that will increase and then decrease in magnitude during the collision, and a frictional part E_f that will always increase in magnitude.

$$\begin{aligned}E_n =& \int \mathbf{u}_o^T\mathbf{M}\mathbf{L}_n\,\mathrm{d}p_n + \int \left(\mathbf{L}_n \pm \mu\mathbf{L}_t\right)^T\mathbf{M}\mathbf{L}_n\,p_n\,\mathrm{d}p_n\\ E_n =& \mathbf{u}_o^T\mathbf{M}\mathbf{L}_2p_n + \frac{1}{2}\left(\mathbf{L}_n \pm \mu\mathbf{L}_t\right)^T\mathbf{M}\mathbf{L}_np_n^2 + E_n^{\mathrm{o}} \qquad (2.21)\end{aligned}$$

The constant of integration E_n^o allows this equation to be applied onward from any point during the collision where the value of E_n is known, such as the point where the friction direction (and thus the equation for E_n) changes. It is initially zero, because the collision has not changed the kinetic energy of the system before any impulse is applied.

The frictional portion may also be expressed similarly, but is not directly relevant to this work. E_f and E_n always sum up to a total of $E = \frac{1}{2}\mathbf{u}^T\mathbf{M}\mathbf{u} - K_i$, the change in kinetic energy of the system due to some intermediate amount of impulse applied to the system during the collision.

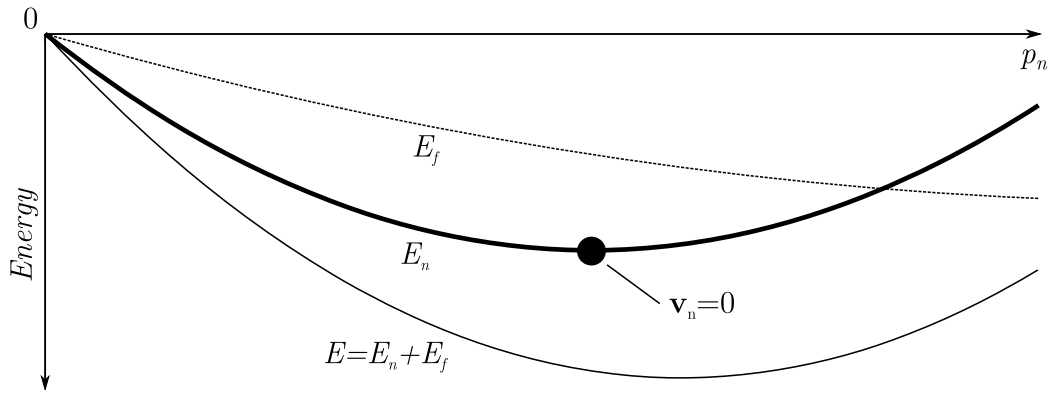

Figure 2.6. Energy exchange during a collision with the separated normal and frictional components.

This splitting of energy allows the energetic COR to be appropriately applied *only to the compressive energy exchange*. Figure 2.6 shows how the kinetic energy of the mechanism changes during a collision, with the portion E_n that goes into compressing the surfaces, and E_f that goes into heat via sliding friction. The point at which compression ends and expansion begins is also shown; it is the extreme point of the E_n curve, where the COR should be applied.

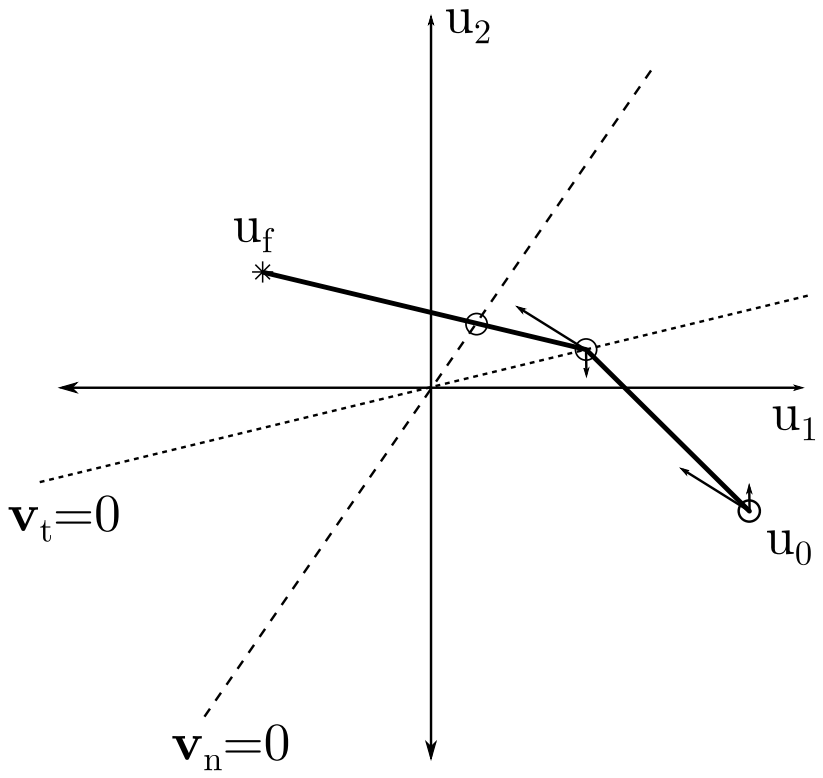

Figure 2.7. Calculating the final energy parameter and velocity state.

In the example collision of Figure 2.7, the dividing point between compression and expansion occurs after the friction direction has changed. At this point, a value for E_n can be calculated based on the total amount of p_n that was required to get there. Then a value of E_n may be obtained for which the collision should end: that is to say, the point at which the impacting surfaces have released all of the stored compressive energy that they will release. This corresponds to the amount of impulse which will separate the colliding surfaces, if they indeed follow the characterization of the energetic COR.

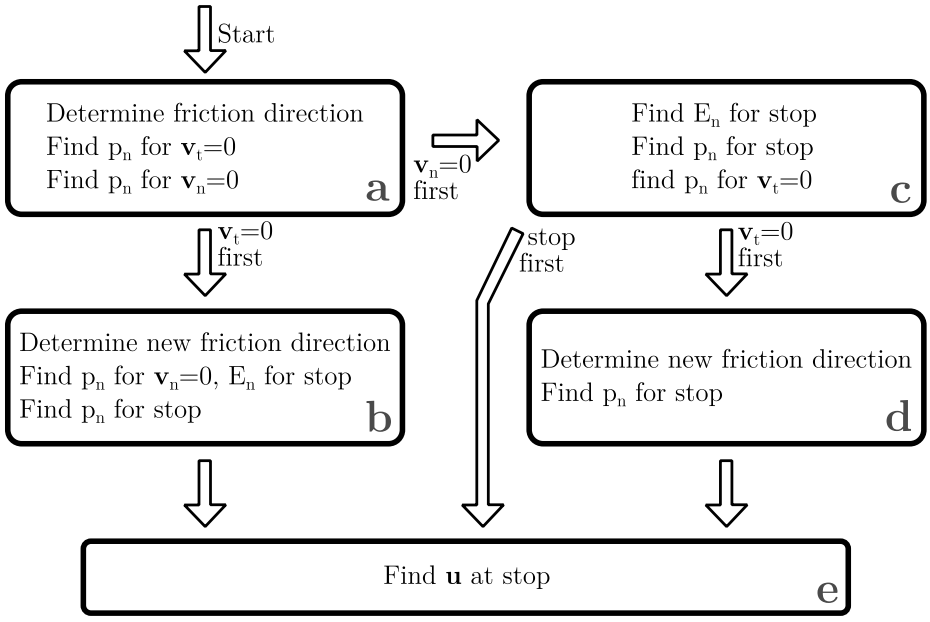

Figure 2.8. A summary of the algebraic algorithm.

There are 3 possible orders in which calculations might be performed, depending on initial configuration and velocity state.

2.3 Algorithm Summary

In this analysis, there are four events of interest during a planar collision. These events correspond to four different generalized speeds along a velocity trajectory that, while discontinuous in time, is continuous in impulse. They are the point where the collision begins, the point where the normal velocity of the collision point is zero, the point where the tangential velocity of the collision point is zero, and the all-important point at which the collision ends.

The middle two points may be solved for algebraically based on the initial velocity and the governing collision equation described in Sec. 2. The tangential "pause" is the location where the sign of the friction force changes; the normal pause is where the compression phase ends and the expansion phase begins. Depending on

which point occurs first (ordered in the impulsive sense), the friction direction may change during the compression phase or the expansion phase.

First, from (2.12), an initial collision direction vector may be found based on the pre-impact velocity and the parameters of the mechanism. This vector defines a line on which all future velocity states during the collision must lie. It is a summation of two vectors: one from normal impulses, and one from tangential impulses.

Next, the two "pause" points may be found at the intersection of the collision line with the hyperplanes representing $\mathbf{v}_t = 0$ and $\mathbf{v}_n = 0$. In this two-degree-of-freedom example, the hyperplanes are also lines. The amount of normal-direction impulse which will push the velocity to each of those two points may also be calculated.

In the example collision, the tangential pause comes first, so path **a-b-e** is followed through the flowchart of Figure 2.8. At the tangential pause, a value for the normal energy exchange parameter E_n may be calculated from (2.21), and stored for continuation of the collision after the collision direction changes. Then (2.12) is applied again to determine a new collision direction, with a changed friction direction. The possibility of sticking is also treated here, in which case the collision will proceed within the hyperplane (along the line) of $\mathbf{v}_t = 0$.

A corrected location and amount of normal impulse is calculated for the normal pause, and E_n is again evaluated. This is the extreme value of E_n, and the moment when the compression phase ends and the expansion phase begins. A stopping value for E_n may be calculated based on this extreme and the coefficient of restitution. Once the stopping value for E_n is known, the normal impulse that will achieve that value may also be found.

Had the normal pause in the example collision occurred first, box **c** would have followed box **a**. The stopping value of E_n would have been calculated before the friction direction change was handled. Figure 2.9 shows examples of two other

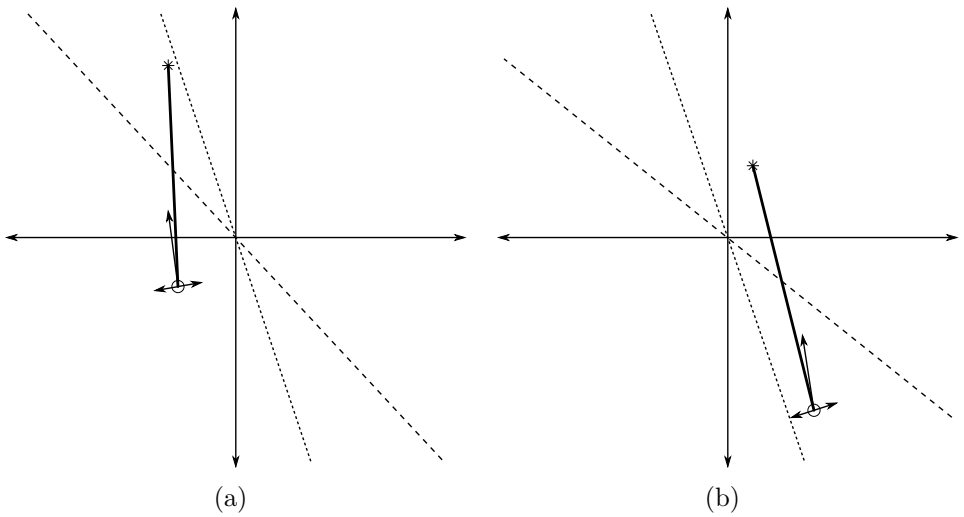

Figure 2.9. Two examples of interesting collision trajectories.

Notation and axes are the same as in Figure 2.7. (a) Collision ends before $\mathbf{v}_t = 0$ is reached. (b) Collision pushes the velocity state entirely away from $\mathbf{v}_t = 0$.

unique cases that may occur, in which no friction direction change happens during the collision. In a case like Figure 2.9 the tangential pause, calculated in the first steps of the algorithm, would go unused, and path **a-c-e** would be taken. In a case like Figure 2.9(b), the value of p_n for the tangential pause will be negative, indicating that it will not occur during the collision. This may also be treated with path **a-c-e**.

Two other special cases are nearly impossible in a collision that results from pre-impact velocities found by numerical integration. The normal and tangential pauses may occur exactly simultaneously, at the point (0,0). In this case, which one is considered first does not matter, because no finite velocity change will occur between the two points. Another rare case occurs if the collision vector $\mathcal{L}$ is exactly parallel to (but not on) the hyperplane $\mathbf{v}_t = 0$. The intersection of the collision line with the hyperplane does not exist in this case, and the calculated value of p_n would

be infinite to push the velocity to an "intersection". This case would be treated the same as the case in Figure 2.9(b).

CHAPTER 3

NOTES ON IMPLEMENTATION

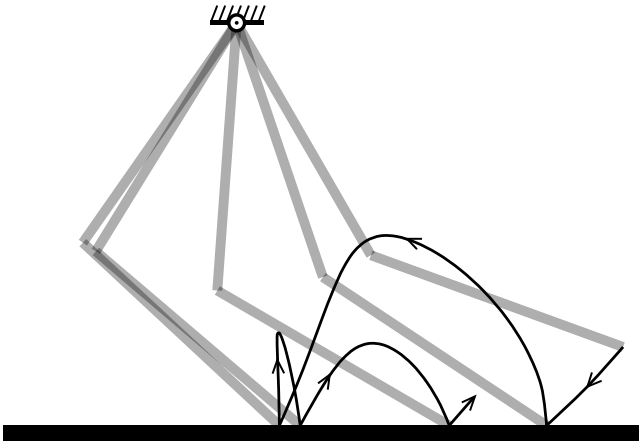

Figure 3.1. Motion of the example mechanism during an actual simulation.

To implement the method of this work on a real system, in order to produce a full motion trajectory prediction as in Figure 3.1, several intersections between lines and hyperplanes must be calculated. For the double pendulum example, these calculations are as follows.

Initially, values for $\mathbf{M}$ and $\mathbf{J}$ are calculated from (2.2) using the values of $\mathbf{q}$ at the impact point/time. A value for m may be obtained before any other calculations

are performed, as the value which will cause the collision vector to lie exactly on the line $\mathbf{v}_t = 0$:

$$m = -\frac{\mathbf{J}_a \mathbf{L}_n}{\mathbf{J}_a \mathbf{L}_t} \tag{3.1}$$

From (2.12), $\mathcal{L}$ may then be determined based on the pre-impact slip direction. The sticking case may be entered during the collision only if $m \leq \mu$. If it is necessary to simulate a difference between static friction and dynamic friction, the static coefficient should be used to determine whether sticking is possible. The dynamic coefficient is used everywhere else.

The pre-impact velocity point and the slope $\mathcal{L}$ define the equation of a line that the velocity will follow as p_n increases. Two points on this line are defined by the intersections with the lines $\mathbf{v}_t = 0$ and $\mathbf{v}_n = 0$. The amount of normal impulse that will push the velocity from some velocity $\mathbf{u}$ to the tangential pause is

$$[p_n|_{\mathbf{v}_t=0}] = -\frac{\mathbf{J}_a \mathbf{u}}{\mathbf{J}_a \mathcal{L}} \tag{3.2}$$

and the amount that will push the velocity to the normal pause is

$$[p_n|_{\mathbf{v}_n=0}] = -\frac{\mathbf{J}_b \mathbf{u}}{\mathbf{J}_b \mathcal{L}} \tag{3.3}$$

If the normal pause occurs first (for a smaller value of p_n, as in Fig. 2.9(a)), the minimum value of E_n may be calculated at that point using (2.21). Then the stopping value of E_n may be calculated using e_*. If the tangential pause occurs first, then the friction direction change must be handled using (2.12). Again, the sticking case may only be entered when $m \leq \mu$.

After the first pause is handled, the second must also be handled. When the second point of interest is the tangential pause (and the friction direction is changed after a stopping value has been calculated for E_n) a new constant of integration E_n^o must be used in (2.21), to enforce continuity of the normal energy parameter. This

new constant of integration should be the value of E_n that was calculated at the tangential pause.

The equations used in this method require the mass matrix to be calculated and inverted, and the Jacobian matrix to be calculated as well. These operations typically require $O(n^3)$ time on the number of generalized coordinates in the system. Since one of the primary motivations for this algorithm is reducing the time required to simulate a collision, it should be noted that an alternative formulation of (2.5) is available.[10] This formulation uses Featherstone's algorithm[5]; it requires only linear time, as it bypasses intermediate calculation of the mass and Jacobian matrices to directly yield the collision matrix L.

CHAPTER 4

TOWARD A FULL THREE-DIMENSIONAL SOLUTION

4.1 Partial Derivation

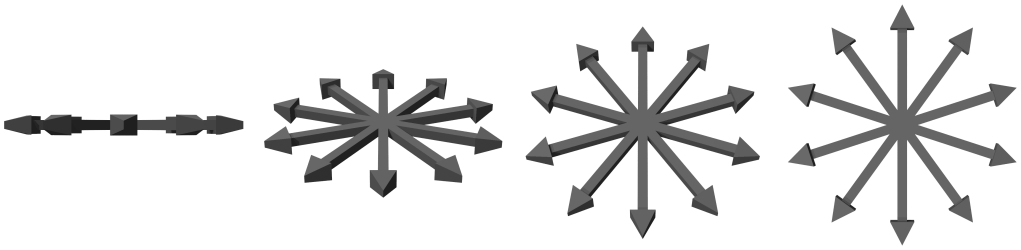

Figure 4.1. Two directions become an infinity of directions.

It usually seems simple to change a derivation from two to three dimensions, but here it is not easy. In order to obtain the solution in Chapter 2, the friction direction was represented simply as the sign, positive or negative, of a frictional influence term. This is possible when the friction force is one-dimensional.

The difference between math in one dimension versus math in two dimensions is very profound, and whole fields of mathematics become suddenly relevant when the jump is made. In this case the primary concern is that the third dimension affects the friction force only, leaving the normal force constrained in it's direction. Suddenly, instead of only two possible friction force directions (+ or -), there are an infinite number of possible directions (illustrated in Figure 4.1).

The analysis in 3D diverges from the 2D analysis at (2.5), where the friction direction may not be simplified down to a sign. Instead of breaking the collision matrix L into two columns and disregarding the third, one must break it into a single

column $\mathbf{L}_n$ that multiplies the normal impulse, and a 3x2 matrix $\mathbf{L}_T$ that multiplies the 2x1 vector $\mathbf{p}_t$ of tangential impulses:

$$\Delta\mathbf{u} = \mathbf{L}_n p_n + \mathbf{L}_T \mathbf{p}_t \tag{4.1}$$

Differentiating by p_n yields

$$\frac{\mathrm{d}\mathbf{u}}{\mathrm{d}p_n} = \mathbf{L}_n + \mathbf{L}_T \frac{\mathrm{d}\mathbf{p}_t}{\mathrm{d}p_n} \tag{4.2}$$

where the differential on the right may be expressed in terms of the normal force f_n (a positive scalar) and the tangential (frictional) force $\mathbf{f}_t$ (a 2x1 vector):

$$\frac{\mathrm{d}\mathbf{p}_t}{\mathrm{d}p_n} = \frac{\dfrac{\mathrm{d}\mathbf{p}_t}{\mathrm{d}t}}{\dfrac{\mathrm{d}p_n}{\mathrm{d}t}} = \frac{\mathbf{f}_t}{f_n} \tag{4.3}$$

For three dimensions, the Coulomb friction equation (2.6) becomes

$$||\mathbf{f}_t|| = \mu ||f_n|| \tag{4.4}$$

This gives the magnitude of the friction force, and its direction is defined to be in the opposite direction from the sliding velocity of the contact point. If the normalized sliding velocity is labeled as a unit vector $\hat{\mathbf{v}}_t$, then (4.3) may become

$$\frac{\mathrm{d}\mathbf{p}_t}{\mathrm{d}p_n} = -\mu\hat{\mathbf{v}}_t \tag{4.5}$$

which yields an expanded form for (4.2):

$$\frac{\mathrm{d}\mathbf{u}}{\mathrm{d}p_n} = \mathbf{L}_n - \mu\mathbf{L}_T\hat{\mathbf{v}}_t \tag{4.6}$$

One last substitution may be performed by recognizing that

$$\mathbf{v}_t = \begin{bmatrix} 1 & 0 & 0 \\ 0 & 1 & 0 \\ 0 & 0 & 0 \end{bmatrix} \mathbf{J}\mathbf{u} \tag{4.7}$$

If a simpler notation is defined as

$$\mathbf{J}_t \equiv \begin{bmatrix} 1 & 0 & 0 \\ 0 & 1 & 0 \\ 0 & 0 & 0 \end{bmatrix} \mathbf{J} \tag{4.8}$$

then (4.6) may be written as

$$\frac{\mathrm{d}\mathbf{u}}{\mathrm{d}p_n} = \mathbf{L}_n - \mu \mathbf{L}_T \frac{\mathbf{J}_t \mathbf{u}}{||\mathbf{J}_t \mathbf{u}||} \tag{4.9}$$

This is an ordinary differential equation in the generalized speeds $\mathbf{u}$. It describes how the velocity of the rigid body system changes during a collision with respect to how much normal impulse has been effected at the contact point. A solution to this differential equation would be a parametric curve having the form

$$\mathbf{u} = f(p_n) \tag{4.10}$$

4.2 Three-Dimensional Algorithm

If a solution in the form of (4.10) were known, a derivation of the energy parameter E_n might be performed, similar to the derivation in (2.15) through (2.21). In the absence of such a solution, numerical integration may be utilized both to generate the parametric velocity trajectory during of the collision and to calculate the value of E_n at each point along that trajectory.

A modified algorithm for solving full 3D collisions may be carried out as follows:

1. Find intersection between velocity trajectory and hyperplane $\mathbf{v}_n = 0$
2. Calculate the value of p_n that yields this intersection
3. Calculate E_n at this intersection
4. Find E_n for end of collision, based on COR
5. Find the value of p_n that yields the stopping value of E_n
6. Use the post-impact velocity state that corresponds to the stopping value of p_n

Sticking may only occur where the velocity trajectory passes *simultaneously* through both of the hyperplanes of zero tangential velocity. For a three-degree-of-freedom system, this would correspond to the intersection between the curve of (4.10) and a line. If this intersection exists within the bounds of the collision, (4.9) may need to be reformulated using the static Coulomb friction model:

$$\mathbf{f}_t = \mathbf{m} f_n : ||\mathbf{m}|| \leq \mu \tag{4.11}$$

This gives a static friction equivalent to(4.9) as:

$$\frac{\mathrm{d}\mathbf{u}}{\mathrm{d}p_n} = \mathbf{L}_n - \mathbf{L}_T\mathbf{m} \tag{4.12}$$

where $\mathbf{m}$ must be chosen such that the vector $\mathbf{L}_n - \mathbf{L}_T\mathbf{m}$ lies simultaneously within both hyperplanes of zero tangential velocity, and $||\mathbf{m}|| \leq \mu$. Integrating this yields the linear post-sticking equation

$$\Delta\mathbf{u} = (\mathbf{L}_n - \mathbf{L}_T\mathbf{m})\, p_n \tag{4.13}$$

Of course, if no such $\mathbf{m}$ exists, sticking is not possible, and the collision trajectory continues in the sliding mode.

CHAPTER 5

CONCLUSIONS

Many methods have been proposed for simulating rigid body collisions, but none have so far been both energetically consistent and closed-form. These characteristics are desirable for use in the simulation of rigid body motion, and this method has both. It does not depend on any tuning or numerical issues associated with numerical methods for integration and optimization. It is numerically precise, requires few calculations, and will yield an answer deterministically.

Future work along this track will require finding a solution to the system of ordinary differential equations given in (**??**). If a solution exists, the method of this work may be easily expanded to cover full three-dimensional collisions between systems of rigid bodies.

REFERENCES

[1] David Baraff. Fast contact force computation for nonpenetrating rigid bodies. In *Proceedings of the 21st annual conference on Computer graphics and interactive techniques*, SIGGRAPH '94, pages 23–34, New York, NY, USA, 1994. ACM.

[2] A. Bowling and D.M. Flickinger. Energetically consistent collisions in simulation of multibody systems. In *Proceedings IEEE International Conference on Robotics and Automation*, pages 1303–1308, May 2009.

[3] A. Bowling and D.M. Flickinger. Simultaneous oblique impacts and contacts in multibody systems with friction. *Multibody System Dynamics*, 23(3):249–261, 2010.

[4] Bernard Brogliato, AA ten Dam, Laetitia Paoli, Frank Génot, and Michel Abadie. Numerical simulation of finite dimensional multibody nonsmooth mechanical systems. *Applied Mechanics Reviews*, 55(2):107–149, March 2002.

[5] R. Featherstone. The calculation of robot dynamics using articulated-body inertias. *The International Journal of Robotics Research*, 2(1):13–30, 1983.

[6] G. Gilardi and I. Sharf. Literature survey of contact dynamics modelling. *Mechanism and Machine Theory*, 37:1213–1239, 2002.

[7] D. T. Greenwood. *Advanced Dynamics*. Cambridge University Press, 2003.

[8] Inhwan Han and B. J. Gilmore. Multi-body impact motion with friction-analysis, simulation, and experimental validation. *Journal of Mechanical Design, Transactions of the ASME*, 115(3):412–422, September 1993.

[9] P. Lötstedt. Numerical simulation of time-dependent contact and friction problems in rigid body mechanics. *SIAM Journal of Scientific and Statistical Computing*, 5(2):370–393, 1984.

[10] Brian Mirtich. *Impulse-based Dynamic Simulation of Rigid Body Systems*. PhD thesis, University of California, Berkeley, 1996.

[11] Inna Sharf and Yuning Zhang. A contact force solution for non-colliding contact dynamics simulation. 16(3):263–290, October 2006.

[12] W. J. Stronge. Friction in collisions: Resolution of a paradox. *Journal of Applied Physics*, 69:610–612, January 1991.

[13] W. J. Stronge. *Impact Mechanics*. Cambridge University Press, 2000. pp. 173-200.

BIOGRAPHICAL STATEMENT

Drew Morgan was born in Fort Worth, TX in 1983. He received his B.S. in Mechanical Engineering in 2006 from California Polytechnic State University, San Luis Obispo, and his M.S. in Mechanical Engineering in 2011 from The University of Texas at Arlington.

Drew worked as an engineer for three companies in Arlington, TX from 2006 to 2009 before starting his M.S work. In addition to his degree in mechanical engineering, he has taken classes in computer science. He has also studied electrical engineering and controls under Dr. Frank Lewis as a member of the Autonomous Systems Lab at the Automation and Robotics Research Institute. His research interests are in control, sensing, and intelligence for autonomous vehicles and robots.